Host–Guest Systems

DOI: 10.1002/anie.201403192

Activation Energies Control the Macroscopic Properties of Physically Cross-Linked Materials**

Eric A. Appel, Rebecca A. Forster, Alexandros Koutsioubas, Chris Toprakcioglu, and Oren A. Scherman

Abstract: *Here we show the preparation of a series of water-based physically cross-linked polymeric materials utilizing cucurbit[8]uril (CB[8]) ternary complexes displaying a range of binding, and therefore cross-linking, dynamics. We determined that the mechanical strength of these materials is correlated directly with a high energetic barrier for the dissociation of the CB[8] ternary complex cross-links, whereas facile and rapid self-healing requires a low energetic barrier to ternary complex association. The versatile CB[8] ternary complex has, therefore, proven to be a powerful asset for improving our understanding of challenging property–structure relationships in supramolecular systems and their associated influence on the bulk behavior of dynamically cross-linked materials.*

A supramolecular perspective has become increasingly important in the design of physically cross-linked materials on account of the explosive growth in the development and understanding of strong and directional noncovalent binding motifs. Specific and well-defined noncovalent interactions, such as hydrogen bonding, host–guest and metal–ligand interactions, can be designed in a rational manner,[1–8] yet little is known about the role of fundamental supramolecular parameters in controlling the macroscopic properties of the resulting materials.[9–11] The advantages of the self-assembly approach to materials lie in the dynamic and stimuli-responsive nature of the interactions that can effectively crosslink functional polymer chains in solution, leading to gel materials that are environmentally responsive in a way that permits tunable, reversible, and self-healing materials.[1–4,6,7,9–12] In these and related materials, macroscopic properties are closely tied to the structure and characteristics of the supramolecular interactions involved in cross-linking.

Many studies have focused on structural manipulations of the supramolecular motifs involved in cross-linking; however, only very few studies have emerged that describe completely and quantitatively the relationship between the fundamental dynamics guiding supramolecular cross-linking and the macroscopic behavior of the resulting materials. This is despite the fact that the lifetime (that is, the dynamic nature) of the supramolecular cross-linking is often the primary attribute distinguishing the resulting materials from their covalent counterparts.[13] Moreover, the dynamics are often central to the function of the supramolecular material as they govern how the structure and properties of the material evolve in response to environmental changes such as mechanical stress, temperature, or other stimuli. Yet, despite their significance, a need still exists to design and execute systematic studies on the complex relationship between the molecular dynamics and bulk mechanical properties of supramolecular polymeric materials.[14,15] Difficulty in characterizing the role of molecular dynamics in the time-dependent micro- and macroscopic properties has arisen from the complicated nature of the determination of kinetics for supramolecular interactions and the design of moieties affording independent control of dynamics and thermodynamics.

Major advancements in the field were made in 2005, when Craig and co-workers published a seminal study demonstrating the use of metal–ligand supramolecular interactions to form cross-linked poly(4-vinylpyridine) (PVP) networks.[3,4] The authors developed a simple bismetallic pincer molecule that utilized small variations in structural steric hindrance to elicit large changes ($\Delta k_{ex} = 10^2\ s^{-1}$) in the exchange kinetics of the bound metal to the pendant pyridine moieties in the PVP, without significantly altering the binding thermodynamics. This remarkable study identified that the bulk material properties in both dynamic and steady shear rheological characterization scaled exactly with the dissociation rate constant, k_d, regardless of the binding thermodynamics (K_{eq}), yielding the broadly applicable principle “strong means slow”, meaning that slow dissociation leads to stronger materials. This scaling with k_d is convenient as the units of the first-order dissociative process (s^{-1}) match those of the experiments and the inverse of k_d (with units of seconds) has been used previously as a measure of the lifetime of the dynamic bond.

Notwithstanding the success of the observations by Craig et al., theoretical treatment of the role of the dynamic noncovalent cross-linking on material properties by Rubinstein and Semenov has been widely supported and focuses primarily on the role of binding thermodynamics on determining material properties.[16] Moreover, the authors’ theo-

---

[*] Dr. E. A. Appel, R. A. Forster, Prof. O. A. Scherman
Melville Laboratory for Polymer Synthesis, Department of Chemistry
University of Cambridge
Lensfield Road, Cambridge CB2 1EW (UK)
Dr. A. Koutsioubas
Synchrotron SOLEIL, Beamline SWING
Saint Aubin BP48, 91192 Gif Sur Yvette Cedex (France)
Prof. C. Toprakcioglu
Department of Physics, University of Patras
Patras 26500 (Greece)

[**] This work was supported by Schlumberger, the Walters-Kundert Foundation, and an ERC Starting Investigator Grant (ASP*i*Re, 240629).

Supporting information for this article is available on the WWW under http://dx.doi.org/10.1002/anie.201403192.

retical treatment begins by defining the lifetime of the dynamic cross-links as scaling with the activation energy of dissociation (Ea_d) in an Arrhenius relationship (where the pre-exponential factor is assumed to be equivalent across all cross-linking moieties), rather than simply the rate constant. Therefore, only very few studies have emerged describing completely and quantitatively the relationship between the fundamental parameters guiding the self-assembly of the supramolecular cross-linking motifs and the macroscopic behavior of the resulting materials. Systematic studies on this complex relationship are highly needed.

Cucurbit[8]uril (CB[8]) is a member of a macrocyclic host family exhibiting a symmetric "barrel" shape with two identical portals that is capable of simultaneously accommodating two guests in a π–π stacked geometry (Figure 1).[17] An electron-deficient guest, such as methyl viologen (MV), and an electron-rich guest form a stable 1:1:1 ternary complex with CB[8] in a stepwise binding process, whereby the electron-poor guest enters the cavity of CB[8] first (K_{eq1}) followed by the inclusion of the electron-rich second guest (K_{eq2}) (Figure 1 b).[17] Exceptionally high overall equilibrium binding affinities ($K_{eq}(\text{total}) = K_{eq1} \times K_{eq2} \leq 10^{14}\,\text{M}^{-2}$) have been reported for these systems,[18] resulting from the energetically favorable replacement of all of CB[8]'s cavity water molecules by the incoming guests.[19] Moreover, as a result of the high binding constants and well-defined ternary complex composition, CB[8] ternary complex formation has been utilized in a number of applications, ranging from the sequence-selective recognition of peptides,[20] surface modifications,[21] protein conjugations[22] to the formation of nanocapsules,[23] nanocomposites,[24] and hydrogels.[6,7,25] It is worth noting, that despite the utility of this binding motif, only one second guest (napthyl derivatives) has been utilized and fundamental knowledge of the binding mechanism and parameters governing complex formation is currently limited to thermodynamics. In many of the above-mentioned applications it would be beneficial if an understanding of the kinetics of the second guest binding event—the essential step to tie together functional entities—could be obtained in order to rationalize the macroscopic behavior of a system. Herein, the association and dissociation dynamics of several second guests binding to the MV⊂CB[8] binary first guest complex are characterized by means of stopped-flow spectrofluorometric experiments. These parameters are then used to rationalize the macroscopic rheological behavior of supramolecular hydrogels prepared by the association of multivalent polymer chains bearing these various second guests and a complementary multivalent first guest polymer in the presence of CB[8].

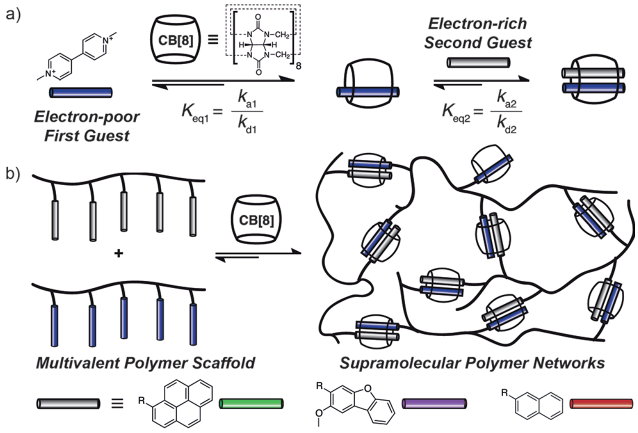

Figure 1. Probing the role of supramolecular dynamics in CB[8]-based physically cross-linked materials. a) Schematic representation of the two-step binding of cucurbit[8]uril with dimethyl viologen (M_2V) and a suitable second guest. b) Multivalent side-chain functional polymers bearing good guests for ternary complex formation with CB[8] form supramolecular hydrogels upon addition of the host molecule.

A series of multivalent random copolymers containing pyrenyl (Pyr), dibenzofuranyl (DBF), and 2-naphthyl (Np) functionality were prepared, each containing the same number of guest moieties (5 % relative to the water-soluble comonomer *N*,*N*-dimethyacrylamide) as well as overall molecular weight ($M_n \approx 50$ kDa) and polydispersity (Table 1). These parameters were particularly important to ensure that beyond the guests themselves no structural variation exists between the guest-functionalized copolymers, in order to minimize any contribution to the hydrogel mechanics not arising exclusively from differences in guest dynamics (see below). Two corresponding multivalent first guest copolymers were prepared according to literature procedures by either post-polymerization conjugation of a methyl viologen species to commercially available poly(vinyl alcohol) (PVA-MV)[7,26] or copolymerization of a methyl viologen functional monomer with a water-soluble comonomer (P(StAM-*r*-StMV)).[6]

Table 1: Characterization of second-guest-functional polymers (PDMAm-G2) used in this study.

Polymer	Guest$_{th}$ [%]	Guest$_{exp}$ [%][a]	M_n [kDa][a]	M_n [kDa][b]	PDI[b]
Np	5.0	5.0	52.2	12.0	1.20
DBF	5.0	5.0	53.1	11.7	1.19
Pyr	5.0	5.0	54.5	11.0	1.19

[a] Determined by ^{1}H NMR spectroscopy. [b] Determined by gel permeation chromatography (GPC) in H_2O.

The association and dissociation kinetic rates of the second guest-functional copolymers (PDMAm-G2) binding to the first guest complex of monovalent small molecule dimethyl viologen and CB[8] (M_2V⊂CB[8]) were then determined by means of stopped-flow experiments. It has previously been demonstrated that these systems do not exhibit multivalent cooperativity[6] on account of the random distribution of guests in the polymer chains; therefore, it is reasonable to utilize the monovalent M_2V⊂CB[8] species to approximate the interactions between multivalent polymers expected during hydrogel formation (see below). Ternary complex formation in these instances is accompanied by fluorescence quenching of the emissive second guest upon binding to M_2V⊂CB[8].[27] Thus, the fluorescent second guests selected were well-suited for this study as a strong quenching of the fluorescence was observed upon addition of $M_2V\subset CB[8]$ to an aqueous solution of PDMAm-G2 polymers. Utilizing a stopped-flow apparatus, the time-dependent fluorescence quenching was observed and fit to a single exponential decay function yielding the observed rate constant (k_{obs}). By altering the molar ratio of $M_2V\subset CB[8]$ to the second guests, with the $M_2V\subset CB[8]$ species in excess, it was possible to invoke pseudo-first order conditions to determine both the associative and dissociative rate constants (k_a and k_d, respectively), according to equation S12 in the Supporting Information.

Both the k_a and k_d values for the ternary complexes at 20 °C were found to vary significantly with second guest structure and electronics, yet the overall equilibrium binding constants (K_{eq2}) were found to be relatively similar for all second guest moieties. Moreover, the K_{eq2} values corresponded well with isothermal titration calorimetry (ITC) measurements for similar multivalent side-chain functional polymers determined previously.[6,7] Furthermore, the stopped-flow experiments were carried out at different temperatures to estimate the Arrhenius activation energies of association (Ea_a) and dissociation (Ea_d) for the ternary complexes from a linear fit of $\ln(k)$ versus T^{-1} in the range of 5–20 °C. The Ea_a values thus determined were similar for all guests, corroborating the previous observations regarding the k_a values. Likewise, the Ea_d values follow the same trend as for k_d, varying amongst the guests, whereby PDMAm-Pyr displays both slower dissociation kinetics and a correspondingly higher energetic barrier to dissociation than the other two guests (Table 2).

Physically cross-linked materials were prepared from multivalent PDMAm-G2 and MV-functionalized polymers in the presence of CB[8]. For example, mixing solutions of PDMAm-G2 with PVA-MV and CB[8] ($PVA\subset CB[8]$) instantaneously formed a brightly-colored hydrogel, the color of which was determined by the charge–transfer (CT) complex between the guest moieties within the CB[8] cavity (Figure 2).[27] A CT-absorption band can be seen for all ternary complexes in the visible region that shifts to longer wavelength with increasing conjugation-length of the second guest, for example, CT $\lambda_{max} = 591$, 445, and 469 nm for PDMAm-Pyr, PDMAm-DBF, and PDMAm-Np, respectively. As observed previously for CB[8]-based hydrogels, their formation is highly specific to the presence of all three components. A lack of any one of them or the replacement of CB[8] with its smaller homologue CB[7] (which forms strong binary complexes with MV) does not lead to cross-linking and gel formation.

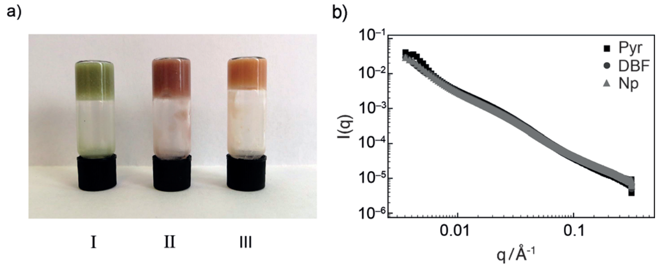

Figure 2. Formation of CB[8]-based physically cross-linked materials. a) Inverted vial test demonstrating hydrogels containing I) PDMAm-Pyr (1 wt%), II) PDMAm-DBF (1 wt%), and III) PDMAm-Np (1 wt%) with PVA-MV (1 wt%) and CB[8] (1 equiv) demonstrating the colors resulting from the charge–transfer complexes occurring between the electron-rich second guests and the electron-poor MV first guest within the CB[8] cavity. b) Small-angle X-ray scattering (SAXS) measurements indicate that the three hydrogels are isostructural, i.e., only differ in the cross-link dynamics due to the various second guests utilized.

Table 2: Kinetic and thermodynamic binding data for multivalent second-guest-functionalized polymers (PDMAm-G2) with $M_2V\subset CB[8]$ in water.

Guest	k_a [10^6; $M^{-1}s^{-1}$][a]	Ea_a [$kJ\,mol^{-1}$]	kd [s^{-1}][a]	Ea_d [$kJ\,mol^{-1}$]	K_{eq} [10^4; M^{-1}][b]
2Np	1.3 ± 0.2	13 ± 2	146 ± 5	30 ± 2	1.5 ± 0.3
DBF	1.5 ± 0.2	10 ± 2	109 ± 5	54 ± 2	1.4 ± 0.2
Pyr	1.1 ± 0.2	10 ± 1	84 ± 4	89 ± 3	1.3 ± 0.2

[a] Values reported for 20 °C. [b] Equilibrium binding constants calculated from the ratio of k_a to k_d obtained at 20 °C.

Small-angle X-ray scattering (SAXS) measurements of these materials were performed to investigate possible gel structural variation arising from the different second guest moieties utilized. Scattering from all samples is identical (Figure 2b), identifying that the materials are isostructural. The scattering data at high q can be described by the Ornstein–Zernike model, which is widely used to account for the scattering from gels and polymeric solutions.[28,29] The high-q data yield a correlation length ξ that could be fitted with values around 8 Å, which is consistent with the calculated mean radius of gyration of chain segments between guest moieties along a polymer chain (≈ 10 Å), whereas the low-q data demonstrate a large degree of forward scattering, likely arising from small amounts of CB[8] (the gels are prepared at the solubility limit of the CB[8]), making it difficult to fit comfortably. The observed lack of structural differences between the materials is important as any differences in the rheological behavior of the hydrogel materials can be explicitly attributed to variation in the dynamics of the CB[8]-based supramolecular cross-links rather than potential differences in the gel structure arising from the use of the different second guests.

Frequency-dependent rheological characterization of these materials performed in the linear viscoelastic region clearly identifies that they are viscoelastic in nature (Figures 3a,b and S4a). In these measurements, both the frequency-dependent rheological data and the plateau modulus are impacted by the formulation (i.e., PVA-MV versus P(StAM- r-StMV)), highlighting that the behavior of the gels can change dramatically with alteration of the polymeric constituents. Materials within a particular composition exhibit roughly identical plateau storage moduli, which is consistent with previous studies demonstrating a correlation between the thermodynamic stability of supramolecular cross-linking motifs (which is equivalent in all gels) in light of the fact that the modulus can be thought of in terms of energy density (that is, energy per unit volume where $1\,Pa = 1\,kJ\,L^{-1}$). The variably dynamic cross-links, however, exhibit a clear effect on the material properties as slower ternary

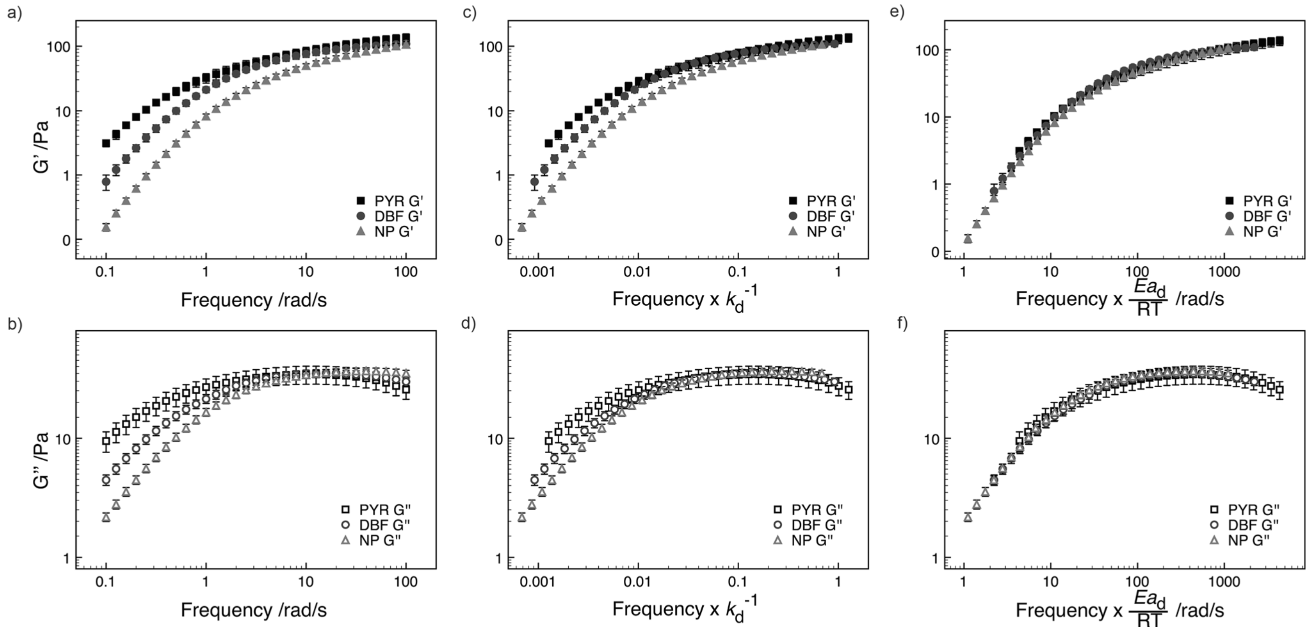

Figure 3. Rheological characterization and scaling of dynamically cross-linked materials. a,b) Frequency-dependent oscillatory rheology of hydrogels prepared from PDMAm-G2 (1.5 wt%), P(StAM-*r*-StMV) (1.5 wt%), and CB[8] (1 equiv). Materials were prepared in triplicate and rheological measurements were performed using a strain of 1% at 20°C. Scaling of the rheological data using c,d) the rate constant of dissociation (k_d) and e,f) a unit-less scaling factor based on the activation energy of dissociation ($\frac{Ea_d}{RT}$) determined for the binding of multivalent side-chain-functionalized PDMAm-G2 polymers with $M_2V\subset CB[8]$.

complex kinetics yield more elastic materials with a crossover between the G' and the G'' at lower frequencies, corroborating previous observations made by Craig and coworkers.[3,4] Furthermore, the dynamics of the supramolecular cross-links apparently play an important role in determining the bulk mechanical behavior as all guests used in this study have equivalent thermodynamic stability, yet their corresponding hydrogels exhibit very different frequency-dependent properties. These observations are similar to those made by Craig et al., yet are in contrast to the assumptions made by Rubinstein and Semenov where a general rule was assumed that thermodynamic stability is directly correlated with small dissociation rate constants and large activation energies for dissociation. In fact, many moieties show slow binding, yet do not possess high thermodynamic stability (for example, the metal–ligand complexes used by Craig et al.), whereas the opposite is true for CB[8]-based complexation, in which the thermodynamic stability is high, yet both the associative and dissociative processes are fast.

Scaling of the rheological data with the kinetic parameters determined for the multivalent second-guest polymers and $M_2V\subset CB[8]$ (Figures 3c,d and Figure S4b), however, identifies a more complicated picture than previously observed by Craig and co-workers.[3,4] Rather than overlaying one another, the respective data do not scale correctly. This lack of agreement is not particularly surprising as the overall dissociation rate constant (k_d) is neither a representation of the energy required when converting an "active" (complexed) cross-link into an "inactive" (uncomplexed) one, nor a measure of the time-dependent distribution of complexed and uncomplexed cross-links. It is intuitive that this conversion might be more appropriately defined by an energetic parameter such as the activation energy for dissociation (Ea_d). Scaling of the data when using the Arrhenius relationship ($\tau = \tau_0 \cdot \exp(\frac{Ea_d}{RT})$) promoted by Rubinstein and Semenov,[16] however, is also unsuccessful. This is perhaps due to the large differences in the pre-exponential factor for the dissociative processes of each second guest determined previously with stopped-flow spectrofluorimetry, highlighting that the dissociative process is second-guest dependent. In contrast, scaling of the frequency-dependent rheological data with unit-less activation energy ($\frac{Ea_d}{RT}$) values determined previously for the multivalent second-guest-functionalized PDMAm-G2 copolymers yields an exact overlay (Figures 3e,f and S4c), demonstrating the normalization of the hydrogel behavior with the supramolecular chemistry responsible for the dynamic cross-linking. Correct scaling is observed regardless of the MV-functional polymer utilized (distinguished by a different molecular weight, polydispersity, persistence length, and functional-group density). Previous researchers have correctly reported that scaling of the viscoelastic properties of dynamically cross-linked materials is controlled primarily by the dissociative process, however, our experiments show that the Ea_d of the dynamic cross-links determines the contribution to material properties of the supramolecular cross-linking, rather than the corresponding k_d.

In order to ensure that our observations were general and not specific for the temperatures used, we repeated the rheological experiments with hydrogels prepared from P(StAM-*r*-StMV) at elevated temperatures. Again, an effective scaling of the data occurs exclusively with the unit-less activation energies of dissociation of the ternary complex cross-links (Figure S5). The disambiguation of kinetic and thermodynamic parameters in our system on account of the differences in structure and electronics of the second guest moieties used in this study, thereby allows for an in-depth and quantitative understanding of the role of such parameters in determining bulk material properties of physically cross-linked materials.

Previous studies on the development of CB[8]-based supramolecular hydrogels found that these materials exhibited extremely rapid self-healing after network rupture by the application of high shear rates in step-shear measurements.[7,30] This feature was proposed to arise from the high association rate constants for the CB[8] ternary complex with Np guests estimated previously.[6] With such a broad range of important kinetic parameters for several second guests and associated hydrogels in hand, this rapid self-healing behavior was herein investigated further. Hydrogels prepared from PDMAm-Pyr, PDMAm-DBF, and PDMAm-Np with PVA-MV⊂CB[8] were first characterized by step-strain measurements, whereby a large-magnitude oscillatory strain (100 %) was applied, immediately followed by a small-magnitude strain (0.1 %). The large-magnitude strain ruptures the hydrogel structure, while the small-magnitude strain allows for the recovery of the material properties, that is, self-healing, which can be observed over time. This method provides an important characterization of the process of self-healing, which occurs only on short time scales after network rupture, as argued by Rubinstein and Leibler,[31] when the concentration of uncomplexed supramolecular moieties is high. The alternative process, self-adhesion, occurs when the concentration of uncomplexed moieties is close to equilibrium.

Unfortunately, the CB[8]-based hydrogels, regardless of the guest, recover their mechanical properties at such a rate that it was impossible to observe the process as the material had completely recovered before the first data point was obtained with step-strain measurements. Step-shear measurements were therefore utilized, whereby a large-magnitude shear rate ($100\,s^{-1}$) was applied, immediately followed by a small-magnitude shear rate ($0.1\,s^{-1}$). With this method, network repair can be monitored in real time. Figure 4 shows the results of these measurements applied over three cycles to each of the three materials at 50 °C. The strength of these hydrogels ($G_0' > 1$ kPa) made it necessary to use higher temperatures to observe the transition, because the hydrogels were expelled from the rheometer geometry at ambient temperatures. Sampling rates are much higher during step-shear measurements than are possible for step-strain measurements, thereby allowing for the collection of data during the entire self-healing process, which is complete in less than 0.5 seconds. Fitting the observed increase in viscosity over time to a one-phase association function yielded the rate constant of self-healing (k_{healing}) for the hydrogels. The obtained values of k_{healing} were independent of the second guest structure and electronics, corroborating observations made previously regarding the kinetics of association for CB[8] ternary complexes with various guests. While previous reports have used these types of self-healing curves to qualitatively describe macroscopic gel behavior, quantitative analysis of this behavior to correlate to molecular parameters has not yet been performed.

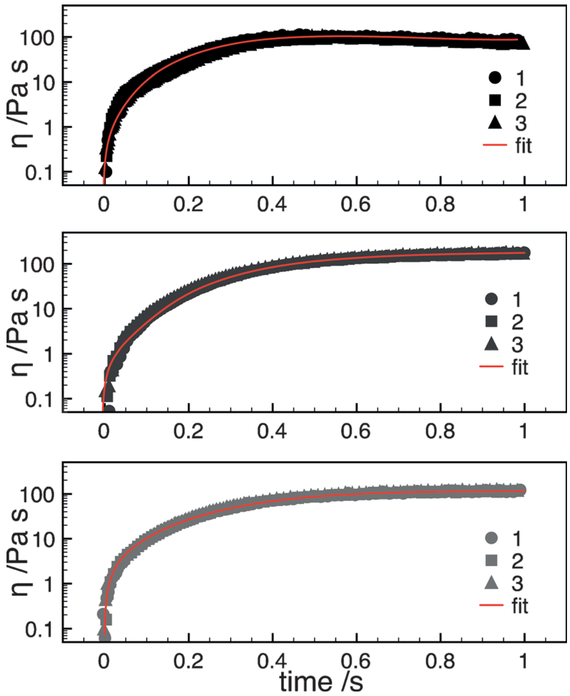

Figure 4. Rapid self-healing of CB[8] cross-linked materials evidenced by step-shear rheological measurements of hydrogels prepared from a) PDMAm-Pyr (1 %), b) PDMAm-DBF (1 %), and c) PDMAm-Np (1 %) with PVA-MV (1 %) and CB[8] (1 %). The plots display only the first 1 s of each of three healing cycles performed at 50 °C yielding healing rate constants (k_{healing}) of 11.5 ± 0.3, 8.0 ± 0.2, and $6.9 \pm 0.2\,s^{-1}$, respectively.

Step-shear experiments were then performed at different temperatures to estimate the Arrhenius activation energies of healing (Ea_{healing}) for the hydrogels. Arrhenius Ea_{healing} values were obtained from a linear fit of $\ln(k_{\text{healing}})$ versus T^{-1} in the range of 40–60 °C. The Ea_{healing} values were also insensitive to the second guest structure and electronics and are in agreement with the values previously determined for the association of PDMAm-G2 to $M_2V{\subset}CB[8]$ ($Ea_{\text{healing}} = 15 \pm 2\,kJ\,mol^{-1}$; see values for Ea_a in Table 2). These observations indicate that the self-healing process for CB[8]-based supramolecular hydrogels is driven primarily by the associative process of the CB[8] ternary complex comprising the dynamic cross-links within the materials, which exhibits an exceedingly low energetic cost, thereby resulting in facile and rapid recovery at room temperature after network damage.

In summary, supramolecular hydrogels have been prepared utilizing the host–guest interactions of a range of guest molecules with the macrocyclic host cucurbit[8]uril. Independent characterization of the molecular kinetics and thermodynamics of the binding of these guest moieties allowed for the elucidation of their impact on the macroscopic properties of the corresponding hydrogels. The energetic barrier to dissociation determines the mechanical strength, whereas the energetic barrier to association determines the capacity of the materials to self-heal, thereby providing a more in-depth picture of the role of supramolecular dynamics and the importance of the energetic barrier for dissociation in determining bulk material properties. The cucurbit[8]uril binding motif has proven to be a powerful asset for improving our understanding of challenging property–structure relationships in supramolecular systems and their associated influence on the bulk behavior of supramolecular cross-linked materials.

Received: March 10, 2014
Revised: June 6, 2014

Keywords: macromolecules · nanomaterials · self-healing · supramolecular polymers

---

[1] M. Lemmers, J. Sprakel, I. K. Voets, J. van der Gucht, M. A. C. Stuart, *Angew. Chem.* **2010**, *122*, 720–723; *Angew. Chem. Int. Ed.* **2010**, *49*, 708–711.
[2] E. Spruijt, J. Sprakel, M. Lemmers, M. A. C. Stuart, J. van der Gucht, *Phys. Rev. Lett.* **2010**, *105*, 208301.
[3] W. Yount, D. Loveless, S. Craig, *Angew. Chem.* **2005**, *117*, 2806–2808; *Angew. Chem. Int. Ed.* **2005**, *44*, 2746–2748.
[4] W. Yount, D. Loveless, S. Craig, *J. Am. Chem. Soc.* **2005**, *127*, 14488–14496.
[5] S. Burattini, B. W. Greenland, D. H. Merino, W. G. Weng, J. Seppala, H. M. Colquhoun, W. Hayes, M. E. Mackay, I. W. Hamley, S. J. Rowan, *J. Am. Chem. Soc.* **2010**, *132*, 12051–12058.
[6] E. A. Appel, F. Biedermann, U. Rauwald, S. T. Jones, J. M. Zayed, O. A. Scherman, *J. Am. Chem. Soc.* **2010**, *132*, 14251–14260.
[7] E. A. Appel, X. J. Loh, S. T. Jones, F. Biedermann, C. A. Dreiss, O. A. Scherman, *J. Am. Chem. Soc.* **2012**, *134*, 11767–11773.
[8] J. R. Capadona, K. Shanmuganathan, D. J. Tyler, S. J. Rowan, C. Weder, *Science* **2008**, *319*, 1370–1374.
[9] S. Seiffert, J. Sprakel, *Chem. Soc. Rev.* **2012**, *41*, 909–930.
[10] E. A. Appel, J. del Barrio, X. J. Loh, O. A. Scherman, *Chem. Soc. Rev.* **2012**, *41*, 6195–6214.
[11] R. J. Wojtecki, M. A. Meador, S. J. Rowan, *Nat. Mater.* **2011**, *10*, 14–27.
[12] J. Wang, D.-T. Main, X. Guo, L. Li, S. F. Lincoln, Z. Luo, H. Ke, L. Zheng, R. K. Prud'homme, *Ind. Eng. Chem. Res.* **2010**, *49*, 609–612.
[13] A. V. Davis, R. M. Yeh, K. N. Raymond, *Proc. Natl. Acad. Sci. USA* **2002**, *99*, 4793–4796.
[14] J. T. Davis, M. S. Kaucher, F. W. Kotch, M. A. Iezzi, B. C. Clover, K. M. Mullaugh, *Org. Lett.* **2004**, *6*, 4265–4268.
[15] A. Hori, K. Yamashita, M. Fujita, *Angew. Chem.* **2004**, *116*, 5126–5129; *Angew. Chem. Int. Ed.* **2004**, *43*, 5016–5019.
[16] M. Rubinstein, A. N. Semenov, *Macromolecules* **2001**, *34*, 1058–1068.
[17] J. W. Lee, S. Samal, N. Selvapalam, H.-J. Kim, K. Kim, *Acc. Chem. Res.* **2003**, *36*, 621–630.
[18] U. Rauwald, F. Biedermann, S. Deroo, C. V. Robinson, O. A. Scherman, *J. Phys. Chem. B* **2010**, *114*, 8606–8615.
[19] F. Biedermann, V. D. Uzunova, O. A. Scherman, W. M. Nau, A. De Simone, *J. Am. Chem. Soc.* **2012**, *134*, 15318–15323.
[20] J. J. Reczek, A. A. Kennedy, B. T. Halbert, A. R. Urbach, *J. Am. Chem. Soc.* **2009**, *131*, 2408–2415.
[21] F. Tian, N. Cheng, N. Nouvel, J. Geng, O. A. Scherman, *Langmuir* **2010**, *26*, 5323–5328.
[22] F. Biedermann, U. Rauwald, J. M. Zayed, O. A. Scherman, *Chem. Sci.* **2011**, *2*, 279–286.
[23] J. Zhang, R. J. Coulston, S. T. Jones, J. Geng, O. A. Scherman, C. Abell, *Science* **2012**, *335*, 690–694.
[24] R. J. Coulston, S. T. Jones, T.-C. Lee, E. A. Appel, O. A. Scherman, *Chem. Commun.* **2011**, *47*, 164–166.
[25] E. A. Appel, X. J. Loh, S. T. Jones, C. A. Dreiss, O. A. Scherman, *Biomaterials* **2012**, *33*, 4646–4652.
[26] F. Biedermann, E. A. Appel, J. del Barrio, T. Gruendling, C. Barner-Kowollik, O. A. Scherman, *Macromolecules* **2011**, *44*, 4828–4835.
[27] F. Biedermann, O. A. Scherman, *J. Phys. Chem. B* **2012**, *116*, 2842–2849.
[28] L. Benguigui, F. Boue, *Euro. Phys. J. B* **1999**, *11*, 439–444.
[29] F. Horkay, P. J. Basser, A. M. Hecht, E. Geissler, *Polymer* **2005**, *46*, 4242–4247.
[30] J. R. McKee, E. A. Appel, J. Seitsonen, E. Kontturi, O. A. Scherman, O. Ikkala, *Adv. Funct. Mater.* **2014**, *24*, 2706–2713.
[31] E. B. Stukalin, L.-H. Cai, N. A. Kumar, L. Leibler, M. Rubinstein, *Macromolecules* **2013**, *46*, 7525–7541.